

SLAC-PUB-8597  
August 2000  
physics/0008195

## **Investigations of Slow Motions of the SLAC Linac Tunnel**

Andrei Seryi

Presented at the 20th International Linac Conference (Linac 2000,  
8/21/2000—8/25/2000, Monterey, CA, USA)

*Stanford Linear Accelerator Center, Stanford University, Stanford, CA 94309*

---

Work supported by Department of Energy contract DE-AC03-76SF00515.

# Investigations of Slow Motions of the SLAC Linac Tunnel \*

Andrei Seryi

Stanford Linear Accelerator Center, Stanford University, Stanford, California 94309 USA

Abstract

Investigations of slow transverse motion of the linac tunnel of the Stanford Linear Collider have been performed over period of about one month in December 1999 – January 2000. The linac laser alignment system, equipped with a quadrant photodetector, allowed submicron resolution measurement of the motion of the middle of the linac tunnel with respect to its ends. Measurements revealed two major sources responsible for the observed relative motion. Variation of the external atmospheric pressure was found to be the most significant cause of short wavelength transverse motion of the tunnel. The long wavelength component of the motion has been also observed to have a large contribution from tidal effects. The measured data are essential for determination of parameters for the Next Linear Collider.

## 1 INTRODUCTION

The electron-positron linear colliders envisioned for the future must focus the beams to nanometer beam size in order to achieve design luminosity. Small beam sizes impose strict tolerances on the positional stability of the collider components, but ground motion will continuously change the component positions.

For linear colliders, the ground motion can be specifically categorized into fast and slow motion. Fast ground motion (roughly  $f \gtrsim 0.1\text{Hz}$ ) causes the beam position to change from pulse to pulse. In contrast, slow ground motion ( $f \lesssim 0.1\text{ Hz}$ ) does not result in an offset of the beams at the interaction point since it is corrected by feedback on a pulse to pulse basis. However slow motion causes emittance dilution since it causes the beam trajectory to deviate from the ideal line. Investigations of slow ground motion are essential to determine the requirements for the feedback systems and to evaluate the residual emittance dilution due to imperfections in the feedback systems.

Investigations of slow motion of the SLAC linac tunnel, described in this paper, were performed in the framework of the Next Linear Collider [1]. The measurements were taken from December 8, 1999 to January 7, 2000. Earlier measurements using the same technique were performed at SLAC in November 1995 for a period of about 48 hours [2]. The goal of the measurements was to systematically study the slow motion and to find correlations with various external parameters in order to identify the driving causes.

## 2 RESULTS AND DISCUSSION

The measurements of slow ground motion were performed using the SLAC linac laser alignment system [4]. This system consists of a light source, a detector, and about 300 targets, one of which is located at each point to be aligned over a total length of 3050 m. The targets are installed in a 2-foot diameter aluminum pipe which is the basic support girder for the accelerator. The target is a rectangular Fresnel lens which has pneumatic actuators that allow each lens to be flipped in or out. The light source is a He-Ne laser shining through a pinhole diaphragm. The beam divergence is large enough to cover even nearby targets and only transverse position of the laser, but not angle, influences the image position. The lightpipe is evacuated to about 15 microns of Mercury to prevent deflection of the alignment image due to refraction in air. Sections of the lightpipe, which are about 12 meters long, are connected via bellows that allow independent motion or adjustment.

A schematic of the measurement setup is shown in Fig.1. The measurements were done with a single lens inserted which was not moved until the measurements were finished in order to ensure maximal accuracy. (In multi target mode the repeatability of the target positioning limits the accuracy). We used the lens 14-9 located at the end of the 14th sector of 30 total, almost exactly in the middle of the linac.

For these measurements, we replaced the standard detector for this system with a quadrant photodetector (produced by Hamamatsu) which has a quadratic sensitive area ( $\sim 10 \times 10\text{ mm}^2$ ) divided into four sectors. By combining preamplified signals  $u_i$  from these quadrants, the quantity to be measured  $X = x_1 + x_3 - 2x_2$  (see Fig.1) can be determined as  $X \propto [(u_1 + u_2) - (u_3 + u_4)]/\Sigma u_i$  for both the horizontal and vertical ( $Y$ ) planes. Calibration of the system was done by moving the detector transversely. The sensitivity is linear in the range of  $\pm 1\text{ mm}$ .

The measured data are shown in Fig.2. Two particular characteristics are clearly seen: the tidal component of the motion is very pronounced and there is a strong correlation of the motion with external atmospheric pressure.

The linac tunnel was closed, with temperature stabilized water through the RF structures during the entire period

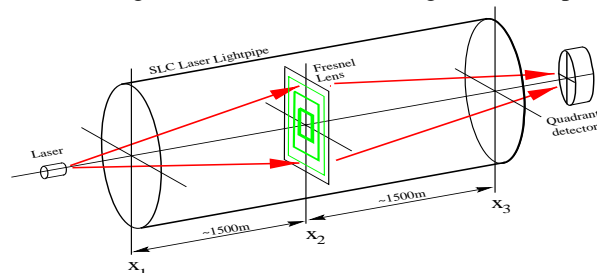


Figure 1: Schematic of the measurement setup.

\* Work supported by the U.S. Department of Energy, Contact Number DE-AC03-76SF00515.

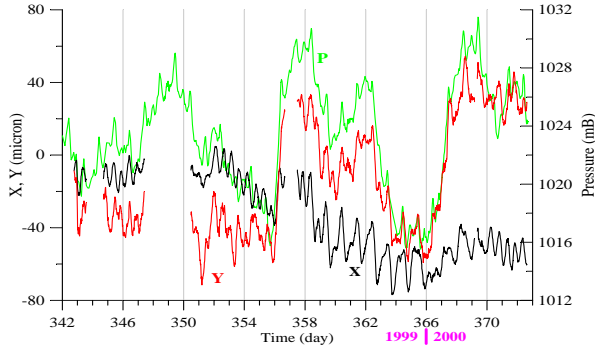


Figure 2: Measured horizontal  $X$  and vertical  $Y$  displacements plotted along with external atmospheric pressure.

of the measurements. The girder temperature was stable within  $0.1^\circ\text{C}$  over a day and within a few  $0.1^\circ\text{C}$  over a week. The RF power was switched off starting Dec. 24 and turned on again Jan. 3. This resulted in a slow (weekly) change of the girder temperature by  $0.5^\circ\text{C}$  in the middle of the linac and  $1.5^\circ\text{C}$  at the beginning. The average external temperature varied by about  $10^\circ\text{C}$  over the month. No significant correlation of the measured data with these and other parameters was observed.

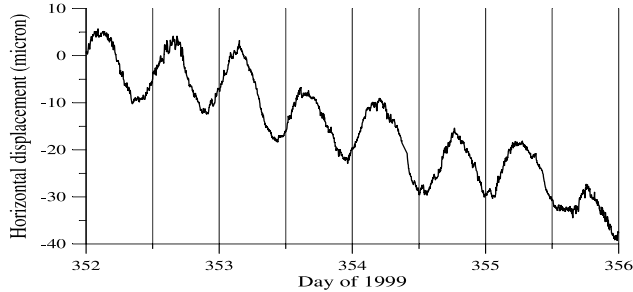


Figure 3: Subset of data where tides are seen most clearly.

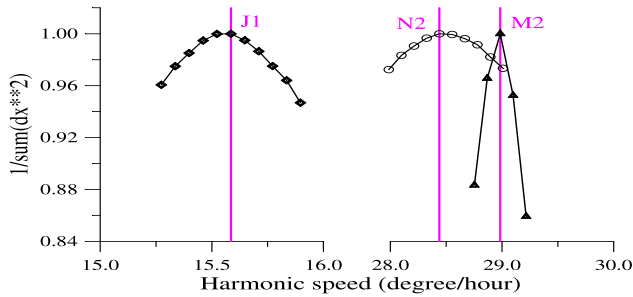


Figure 4: Normalized  $1/\chi^2$  showing quality of fit of the measured data by sum of 37 tidal harmonics. Behavior of  $1/\chi^2$  if the speed of one harmonic would vary. Example for the harmonics M2 (principal lunar), N2 and J1. Vertical lines show theoretical speed of these harmonics.

The tidal component of the motion has a surprisingly large amplitude ( $\sim 10\mu\text{m}$ ) (see Fig.3). The most pronounced harmonics in the measured data are M2 (principal lunar), N2 and J1. The primary effect of tidal deformation is to change the slope of the earth's surface ( $\sim 100\mu\text{m}/1\text{km}$  assuming total deformation  $\sim 0.5\text{m}$ ). The secondary effect is to change the curvature of the surface ( $\sim 0.01\mu\text{m}/1\text{km}^2$  if one assumes uniform earth deformation). The laser system is not sensitive to the slope change, but only to the cur-

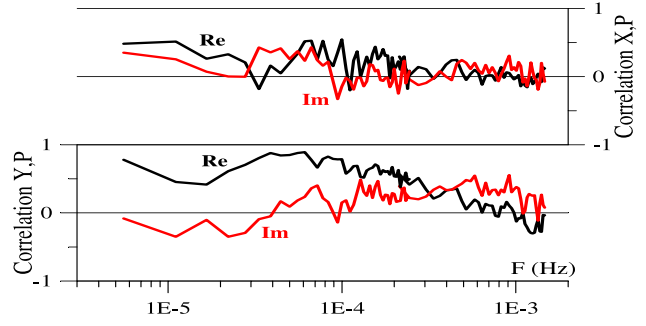


Figure 5: Correlation (real and imaginary parts) of displacement with atmospheric pressure.

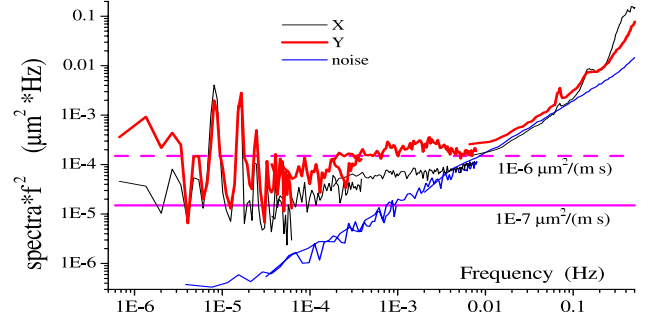


Figure 6: Spectra of displacement (multiplied by  $f^2$ ) and the noise of electronics. Peaks around  $10^{-5}$  Hz correspond to tides. Horizontal lines correspond to the ATL spectra.

vature change, which is an advantage. The observed  $10\mu\text{m}$  change of the curvature can only be explained if a local effect of the tides, with  $R_{\text{effective}} \sim 500\text{km}$ , is assumed. This local anomaly at SLAC is caused by loading on the coastline as the ocean water level varies due to the tides. This phenomenon has been known for many years and is called ocean loading. This effect is also responsible for an enhancement of the tidal variation of the earth surface slope observed in the San Francisco Bay Area [5]. The ocean loading effect vanishes away from the coastline. Regardless, these tidal effects are harmless for a linear collider, because the motion is slow, very predictable and, most importantly, has a wavelength much longer than the length of the accelerator.

Correlation of the tunnel deformation with changes of external atmospheric pressure, clearly seen in Fig.2 and 5, is significant from the lowest observed frequency up to  $\sim 0.003\text{Hz}$ . Above this frequency the characteristic size over which the pressure changes, which is  $\sim v_w/f$ , where  $v_w$  is the wind velocity (typically  $5\text{m/s}$ ), becomes shorter than the linac length and the correlations vanish. In this frequency range, the ratio of deformation to pressure is almost constant at about  $6\mu\text{m}/\text{mbar}$  in  $Y$  and  $2\mu\text{m}/\text{mbar}$  in  $X$ . The influence of such global changes of pressure on the ground deformation can be explained if the landscape or the ground properties vary along the linac. One should note that deformations of the lightpipe itself or motion of the targets caused by external pressure variation appear to be eliminated by design [4].

The spectra of the tunnel deformations exhibits  $1/f^2$  behavior over a large frequency band (see Fig.6). The  $1/f^2$

behavior vanishes at  $f \gtrsim 0.01$  Hz where the signal to noise ratio becomes poor due to noise in the detector and electronics. Evaluation of this noise, also shown in Fig.6, has been done by means of a light source attached directly to the photodetector. The spot size and intensity of this light source were very similar to those of the laser. Influences of other sources of error (vacuum and temperature variation in the lightpipe, temperature in the tunnel, etc.) were analyzed but were found to be insignificant.

Above 0.1 Hz the signal to noise ratio again becomes good as seen in the Fig.6. This is also confirmed by comparison of the measured lightpipe displacement with measurements from a vertical broadband (0.01-100Hz) seismometer STS-2 installed at the beginning of the linac, which measures the absolute motion of the ground. The simultaneous measurements of the tunnel motion and of the absolute motion by STS-2 were performed during 3 days from January 4 to January 7. The coherence between STS-2 and vertical displacement measured by photodetector was found to be about 0.5 at  $F \gtrsim 0.2$  Hz.

During the 3-day period when the tunnel motion was measured simultaneously with STS-2, only two remote earthquakes were detected by the seismometer. One of the earthquakes did not produce any noticeable effect on the motion measured by the photodetector, probably because of the specific orientation of the waves. The second earthquake, however, was clearly seen in both signals, as shown in Fig.7. The ratio of the measured absolute motion and the relative deformation of the tunnel is consistent with a phase velocity of about 2.5 km/s, consistent with earlier correlation measurements performed at SLAC [1].

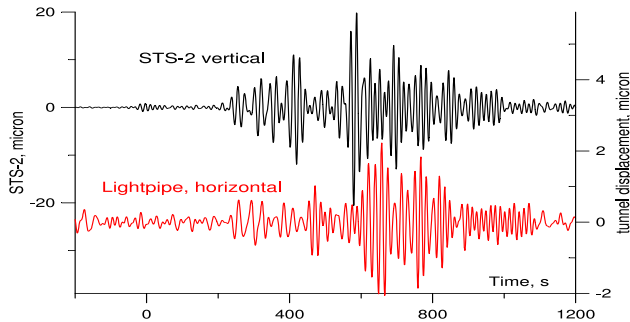


Figure 7: Displacement of the tunnel and displacement measured by STS-2 seismometer during remote earthquake started January 6, 2000 at 02:49:00 local time (supposedly corresponds to 5.8MS earthquake at Alaska happened at 10:42:27 UTC). A passband filter 0.02–0.08Hz has been applied to the data.

One model of slow ground motion is described by the ATL-law [3]. For our 3 point motion, the ATL spectrum corresponding to the measured  $X$  or  $Y$  is  $P(\omega) = \frac{4AL}{\omega^2}$  with  $L = 1500$ m. Fig.6 shows that the measured spectrum corresponds to a parameter  $A$  of about  $10^{-7}$ – $2 \cdot 10^{-6}$   $\mu\text{m}/(\text{m}\cdot\text{s})$ , somewhat changing with frequency.

Spectral analysis of subsets of the data, however, shows that this parameter actually varies in time (see Fig.8). The variation of atmospheric activity is again responsible for

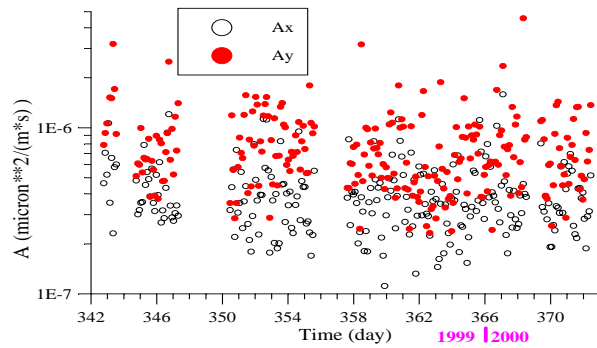


Figure 8: Parameter  $A$  defined from fit to spectra in the band  $2.44\text{E-}4$  to  $1.53\text{E-}2$  Hz for all data.

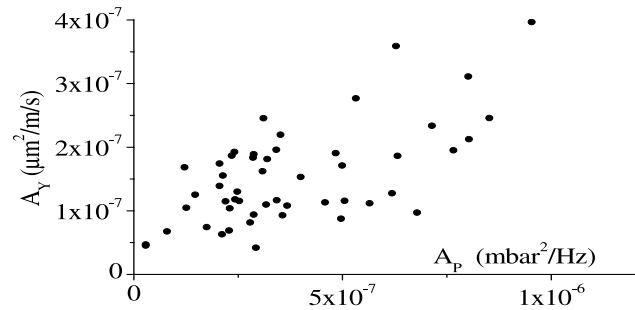


Figure 9: Parameter  $A_y$  defined from all vertical motion data in the frequency band  $3 \cdot 10^{-5}$ – $10^{-3}$  Hz versus amplitude  $A_p$  of the atmospheric pressure spectrum.

the variation of parameter  $A$ . The spectra of pressure fluctuations was found to behave also as  $A_p/\omega^2$  and its amplitude  $A_p$  correlates with the parameter  $A$ , as seen in Fig.9. The temporal pressure variation can therefore be a major driving term of the  $A/\omega^2$ -like motion. This effect strongly depends on geology [7].

### 3 CONCLUSION

Atmospheric pressure changes were found to be a major cause of slow motion of the shallow SLAC linac tunnel. In deep tunnels or in tunnels built in more solid ground, this mechanism would vanish, as it and location. Other sources could then dominate.

I would like to thank G.Bowden, T.King, G.Mazaheri, M.Ross, M.Rogers, L.Griffin, R.Ruland, R.Erickson, T.Graul, B.Herrmannsfeldt, R.Pitthan, C.Adolphsen, N.Phinney and T.Raubenheimer for help, technical assistance and valuable discussions.

### 4 REFERENCES

- [1] NLC ZDR Design Group, SLAC Report-474 (1996).
- [2] C. Adolphsen, G. Bowden, G. Mazaheri, in Proc. of LC97.
- [3] B.Baklavov, P.Lebedev, V.Parkhomchuk, A.Seryi, A.Sleptsov, V.Shiltsev, Tech. Phys. **38**, 894 (1993).
- [4] W. B. Herrmannsfeldt, IEEE Trans. Nucl. Sci. **12**, 9 (1965).
- [5] Milton D. Wood, Ph.D. thesis, Stanford, May 1969.
- [6] R. Assmann, C. Salsberg, C. Montag, SLAC-PUB-7303, in Proceed. of Linac 96, Geneva, (1996).
- [7] A. Seryi, EPAC 2000, also in these Proceed.